Delay-dependent stability for transparent bilateral teleoperation system: an LMI approach

A. Khosravi[1*], A.R. Alfi[2], A. Roshandel[1]

1. Department of Electrical and Computer Engineering, Babol University of Technology, School of Computer Engineering
2. Faculty of Electrical and Robatic Computer Engineering, Shahrood University of Technology, Iran

Abstract

There are two significant goals in teleoperation systems: Stability and performance. This paper introduces an LMI-based robust control method for bilateral transparent teleoperation systems in presence of model mismatch. The uncertainties in time delay in communication channel, task environment and model parameters of master-slave systems are called a model mismatch. The time delay in communication channel is assumed to be large, unknown and asymmetric, but the upper bound of the delay is assumed to be known. The proposed method consists of two local controllers. One local controller namely local slave controller is located on the remote site to control the motion tracking and the other one is located on the local site namely local master controller to preserve the complete transparency by ensuring force tracking and the robust stability of the closed-loop system. To reduce the peak amplitude of output signal respect to the peak amplitude of input signal in slave site, the local slave controller is designed based on a bounded peak-to-peak gain controller. In order to provide a realistic case, an external signal as a noise of force sensor is also considered. Simulation results show the effectiveness of proposed control structure.

Keywords:*Bilateral teleportation system, Complete Transparency, Robust control, Large Time Delay, Linear MatrixInequality.*

1. Introduction

It is common that timedelay is often a source of instability and/or poor performance of many systems. Therefore, stability analysis and control design problems of the time delay systems have drawn an increasing attention during the last two decades. Bilateral teleoperation system is one of the most well-known areas of such systems. In bilateral teleoperation, a human operator applies force to the master in order to produce the desired motion. The motion of master is transmitted to the slave system a communication channel. The slave system tracks the motion of master system and sends back the reflected force from task environment to the master. Bilateral teleoperation system can be generically described by means of the block diagram shown in Figure 1.

Transparency is the major criterion for the performance of teleoperation systems. If the slave accurately reproduces the master's commands and the master correctly feels the slave forces, then the human operator experiences the same interaction as the slave would. This is called transparency in teleoperation systems [1]. In other words, the ideal responses (i.e. the complete transparency) for the teleoperation system with time delay can be defined as follows:
- The force that the human operator applies to the master robot is equal to the force reflected from the task environment. This can help the operator to realize the force sensation.
- The master position/velocity is equal to the slave position/velocity.

Because of the importance of stability and transparency in bilateral teleoperation systems, several control schemes have been proposed in literatures [2]-[18]. Some researchers have analyzed the transparency of teleoperation systems, when there is no time delay in communication channels. Moreover, in some cases, in order to make the system transparent, acceleration of the master and the slave must be sent to the other side. However, acceleration measurement is not an easy task [2]-[7]. In some papers, it has been assumed that the time delay in communication channel is constant [8]-[12]. In addition, some proposed methods in literatures are not stable for large time delays (with or without uncertainties in the time delay) [13]-[16]. Moreover, in some articles, the forward and the backward time delays have been assumed identical [8], [13], [17]-[23]. Some researchers have also proposed different control strategies, such as three and four-channel control methods for teleoperation systems in presence of the time delay with good transparency. Nevertheless, these methods are difficult to realize [24]. In [25] and [26], a simple structure design proposed for bilateral transparent teleoperation systems in presence of time delay uncertainty. In the proposed control method, to achieve complete transparency, direct-force measurement-force reflecting control has been used.
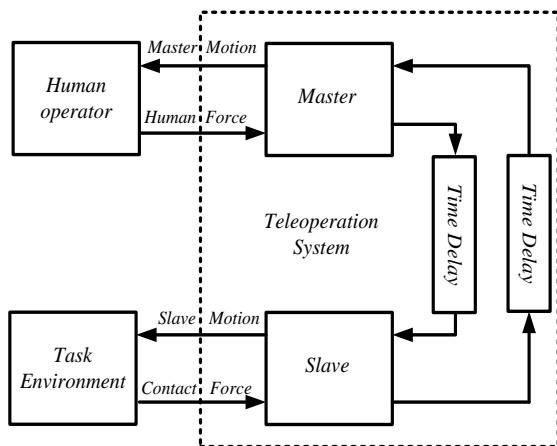

Figure 1. A general framework of bilateral teleoperation system.

Recently, the LMI-based approaches have been employed to deal with stability and stabilization problems [27] such as teleoperation systems. In 2008, an LMI approach to robust H_∞ and L_1 controllers design for a bilateral teleoperation system introduced [28]. Although the time delay of communication channel was assumed to be large, unknown and randomly time varying, but the upper bounds of the time delay interval and the derivative of the delay were assumed to be known. In 2009, the teleoperation system with asymmetric time delays has been also studied in the form of LMI [29]. The stability condition based on LMI has been used to optimize the allowable maximum delay values. In this method, the upper bounds and the derivative of time delay have been assumed to be known. The main drawback of these papers is that the complete transparency has not been achieved.

It is noticeable that there are two different methods to investigate the stability of delay systems: 1) delay-independent stability and 2) delay-dependent stability [30]. The delay-independent stability is defined for any length of nonnegative delay values, while the delay-dependent stability is referred to as the property in which the system is stable for any time delay values as long as $T \leq T_{max}$. So, the delay-dependent stability criterion assumes prior knowledge on the upper bounds of the delay values.

This paper presents a novel LMI-based robust control design for bilateral teleoperation systems in presence of model mismatch. Also, the uncertainties in time delay in communication channel, task environment and model parameters of master-slave systems are called model mismatch. The main goals of the proposed control method are: 1) the closed-loop control system is delay-dependent stable with asymmetric time delays while the whole system is complete transparent; 2) the motion/force scaling can be selected arbitrarily. In other words, it is applicable to micro-micro manipulation. In the proposed method, the time delay in communication channel is assumed to be unknown, but the upper bound of delay is assumed to be known. This assumption is very general for the time delay. Since the time delay of the practical systems are often bounded, it is reasonable to assume the upper bound on the time delay. To achieve these goals, the proposed method consists of two local controllers. One local controller namely local slave controller is located on the remote site to control the motion tracking and the other one is located on the local site namely local master controller to preserve the complete transparency by ensuring force tracking and the robust stability of the closed-loop system. By applying an LMI-based convex optimization method, a time response can be achieved with smaller settling time accompanied by lower control efforts in local and remote sites.

This paper is briefly outlined as follows: the modeling of bilateral teleoperation systems including time delay in communication channel is presented in section II. Section III introduces the standard representation of control system. The main results are represented in section IV. This section is assigned to the design of local controllers. The stability analysis of the proposed control structure is also described. Section V shows the simulation results. Finally, section VI draws conclusions and gives some suggestions for the future works.

2. System description
2.1.Structure of teleoperation system
Figure 2 depicts the structure of bilateral teleportation system. In this figure, G is the transfer function of the system, C shows the local controller, indices m and s denote the master and the slave systems, respectively, f_e is the contact force from task environment,f_r is the reflected force from the remote environment, f_h demonstrates the force applied to the master system by the human operator, T_{ms} and T_{sm} are the forward (from master to slave) and backward (from slave to master) time delays, respectively. Moreover, Z_e is the impedance of the task environment and $v(t)$represents the sensor noise of the force measurement in the remote site. Finally, K_p and K_f are the arbitrary motion and force scaling factors, respectively.
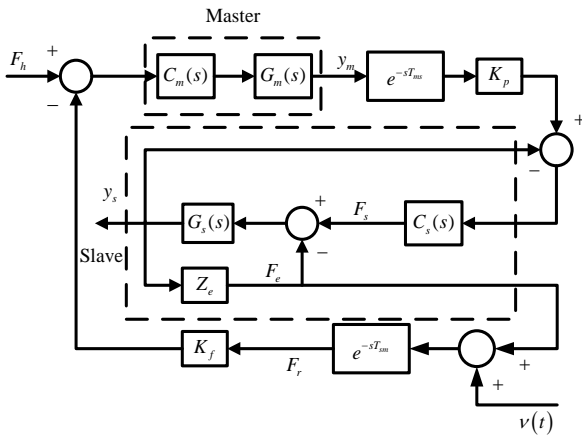

Figure 2. Teleportation system structure.

It is noticeable that because of using direct-force measurement-force reflecting control, the utilization of force sensor is inevitable. Hence, the noise of sensor in the remote site must be considered. This issue has not been investigated in

[25], [26]. The following assumptions have to be stated first:

Assumption 1: The forward and backward time delays are assumed to be bounded and can be non-identical.

Assumption 2: The slave system acts on hard task environment.

Assumption 3: The contact force f_e is measurable.

2.2.Modeling of time delay
In the proposed control methodology, the time delay uncertainty is modeled in multiplicative form. According to assumption 1, a new bounded variable denoted by T can be defined as a summation of the forward and the backward time delays.

$$T = T_{ms} + T_{sm}, \quad 0 \leq T \leq T_{max} \tag{1}$$

Based on fluid flow model [31], the time delay T can be represented as follows:

$$T = \frac{1}{2}(T_{max} + T_{min}) + \frac{1}{2}(T_{max} - T_{min})\beta, \qquad -1 \leq \beta \leq 1 \tag{2}$$

Where T_{max} and T_{min} are the upper bound and the lower bound of T, respectively and the parameter β specifies the uncertainty region. Let define a new parameter γ as

$$\gamma = \frac{1}{2T_{max}}(T_{max} - T_{min}) \tag{3}$$

Substituting (3) into (2) yields

$$T = (1-\gamma)T_{max} + \gamma T_{max}\beta, \quad \circ \leq \gamma \leq 0.5 \tag{4}$$

The parameters β and γ are real constants to be determined based on application. The first term of (4) shows a constant delay part while the second term represents the uncertain delay time. By using the first-order Pade′ approximation, the exponential delay transfer function is written as

$$e^{-sT} = e^{-s(1-\gamma)T_{max}} e^{-s\gamma\delta T_{max}} \cong \frac{1 - sT/2}{1 + sT/2} \tag{5}$$

$$\approx \left(\frac{1 - s(1-\gamma)T_{max}/2}{1 + s(1-\gamma)T_{max}/2}\right)\left(\frac{1 - s\gamma T_{max}\beta/2}{1 + s\gamma T_{max}\beta/2}\right)$$

Hence, the uncertain delay part given in (5) can be expressed as a multiplicative uncertainty.

$$\frac{1-s\gamma T_{\max}\,\beta/2}{1+s\gamma T_{\max}\,\beta/2}=1-\frac{s\gamma T_{\max}\,\beta}{1+s\gamma T_{\max}\,\beta/2} \qquad (6)$$

$$=1+W_{mT}(s)\Delta$$

Where Δ is the perturbation function with $\|\Delta\|_{\infty}<1$ and

$$W_{mT}(s)=\frac{s\gamma T_{\max}\,\beta}{1+s\gamma T_{\max}\,\beta/2} \qquad (7.1)$$

is a multiplicative uncertainty weigh. As $W_{mT}(s)$ cannot cover all possible uncertain delay, the following modified weighting function is used [32]:

$$W_{mT}(s)=\frac{s\gamma T_{\max}\,\beta}{1+s\gamma T_{\max}\,\beta/3.465} \qquad (7.2)$$

Figure 3 shows the configuration of time delay uncertainty used in this paper. It should be noted that the lower bound of time delay is also frequently equal to zero.
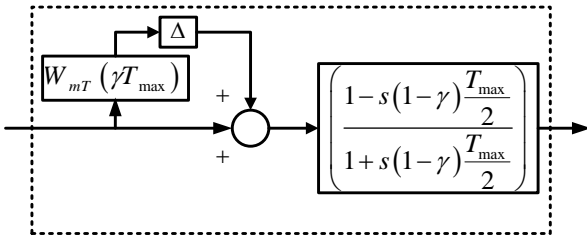
Figure 3. Configuration of time delay uncertainty

3. Standard representation of control system

Figure 4 shows the standard control representation for the local controllers design, i.e. local master controller C_m and local slave controller C_s. In this figure, u is the control input, w is a vector of exogenous signal (reference input signal, disturbance and sensor noise signals) and y is the measurement output signal. Z is also a vector of output signals $(z_1\ z_2\ \dots\ z_i)^T$ related to the performance of the control system. The state space of the structure shown in Figure 4 is defined as follows:

$$\dot{x}=Ax+B_w w+Bu \qquad (8)$$
$$Z=C_z x+D_{zw}w+D_z u$$
$$y=Cx+D_w w$$

Our goal is to find a dynamical output-feedback controller with state space realization given in (9) such that makes desired changes in the outputs' vector.

$$\dot{\zeta}=A_K\zeta+B_K y \qquad (9)$$
$$u=C_K\zeta+D_k y$$

In (9), ζ represents a vector of the controller's states and u and y were introduced before.

Next section presents how we can obtain the structure shown in Figure 4 for local master and slave controllers design.
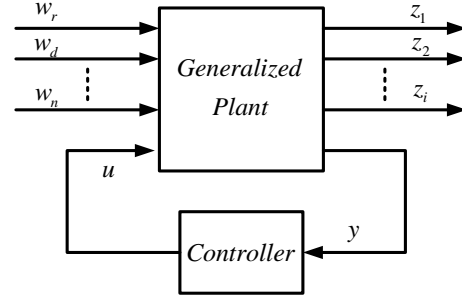

Figure 4. Standard control system representation.

4. Controller design

This section is assigned to the local controllers design. As mentioned before, to achieve robust stability and complete transparency, two local controllers are designed: One controller in the remote site C_s namely local slave controller, and the other in the local site C_m namely local master controller. The local slave controller is responsible for tracking the master commands and the local master controller is in charge of force tracking as well as guaranteeing the robust stability of the closed-loop system. Without loss of generality, the position of master and slave systems are considered. The scaling factors betweenmaster and slave are also set to unity. It should be recalled that the designer can select arbitrary values for motion/force scaling.

4.1. The local slave controller

First, in order to design the local slave controller, the slave control system is reformulated in such a way that it is converted to an equivalent block diagram in a standard control system representation given in Figure 4. Let define the following variable

$$G_s'(s)=\frac{G_s(s)}{1+Z_e G_s(s)} \qquad (10)$$

Hence, referring Figure 2, the standard of slave control system can be shown as Figure 5. Base on control theory, the feedback control system in Figure 5 can be shown as the standard control system representation in Figure 4.
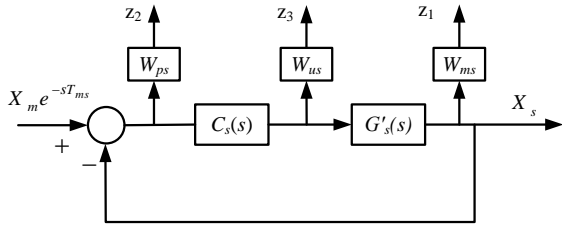
Figure 5. The structure of local slave controller design

In Figure 5, C_s is the local slave controller; W_{ms} is the uncertainty weighting function due to variations in the dynamics of the slave system. W_{ps}, and W_{us} are also the performance and the controller weighting functions, respectively. In addition, motion tracking, to reduce the peak amplitude of output signal respect to the peak amplitude of input signal, a bounded peak-to-peak gain controller for the slave system can be constructed from Theorem 1. The peak-to-peak gain for a transfer function; G_i is defined as [33]:

$$\left\| G_i \right\|_{peak} := sup \left\{ \begin{array}{l} \left\| z_j \left(T\right) \right\| : x_{cl}\left(0\right)=0, T \geq 0, \\ \left\| w_i\left(t\right) \right\| \leq 1 \, for \, t \geq 0 \end{array} \right\} \quad (11)$$

Where x_{cl} denotes the closed-loop state vector. This relation measures the maximum norm of output signal z_j for inputs w_j whose amplitude does not exceed one. Recall that there is no exact characterization for the peak-to-peak norm in the LMI framework, but it is possible to deduce the upper bounds for $\left\| G_i \right\|_{peak}$ [33].

Theorem 1: Consider the closed-loop system in Figure 5. Motion tracking with lower maximum overshoot via local slave controller C_s can be met by solving the following minimization LMI. Based on this, a bounded peak-to-peak gain controller can be constructed for the slave system if there exist X, Y, μ, λ and ζ as follows [33]:

mininmize $\lambda > 0$,

$$\begin{pmatrix} \Pi_{11}+\lambda X & * & * \\ \Pi_{21}+\lambda I & \Pi_{22}+\lambda Y & * \\ \Pi_{31} & \Pi_{32} & -\mu I \end{pmatrix} < 0,$$

$$\begin{pmatrix} \lambda X & \lambda I & 0 & * \\ \lambda I & \lambda Y & 0 & * \\ 0 & 0 & (\zeta-\mu)I & * \\ \Pi_{41} & \Pi_{42} & \Pi_{43} & \zeta I \end{pmatrix} > 0$$

(12)

where Π_{11}, Π_{21}, Π_{31}, Π_{22}, Π_{41}, Π_{32}, Π_{42}, Π_{43} can be obtained from

$$\Pi_{11} := AX + XA^T + B\hat{C}_k + \left(B\hat{C}_k\right)^T \quad \Pi_{21} := \hat{A}_k + \left(A+B\hat{D}_kC\right)^T \quad (13)$$

$$\Pi_{22} := \hat{A}^T Y + YA + B\hat{C}_k + \left(B\hat{C}_k\right)^T \quad \Pi_{32} := \left(YB_w + \hat{B}_k D_w\right)^T$$

$$\Pi_{43} := D_{z_1 w} + D_{z_1}\hat{D}_k D_w \quad \Pi_{41} := C_{z_1}X + D_{z_1}\hat{C}_k$$

$$\Pi_{31} := \left(B_w + B\hat{D}_k D_w\right)^T \quad \Pi_{42} := C_{z_1} + D_{z_1}\hat{D}_kC$$

*sign is used to show the transpose components while A, B_w, C_z and D_{zw} and D_{zw} are related matrices to the desired output channel from the state space realization of the generalized plant, and $\hat{A}_k$, $\hat{B}_k$, $\hat{C}_k$ and $\hat{D}_k$ represent the transformed parameters of the local slave controller which used in order to preserve the linearization of the design problem. If λ is chosen as a positive constant, the minimization of ζ will be a convex optimization. The real parameters of the controller can be constructed from the following relations [33]:

$$D_k := \hat{D}_k \quad (14)$$

$$C_k := \left(\hat{C}_k - D_k CX\right)M^{-T}$$

$$B_k := N^{-1}\left(\hat{B}_k - YBD_k\right)$$

$$A_k := N^{-1}\left(\hat{A}_k - NB_kCX - YBC_kM^T - Y\left(A+BD_kC\right)X\right)M^{-T}$$

Where N and M are nonsingular matrices that should satisfy $MN^T = I - XY$.

4.2. The local master controller

Considering the uncertainty in the time delay as well as the measurement noise accompanied by the reflected force, utilization of a multi-objective H_2/H_∞ controller in the master side is inevitable. The roles of local master controller $C_m(s)$ are to provide robust stability to the overall system and ensure the force tracking based on multiobjective H_2/H_∞ approach. The force tracking means that the reflecting force F_e has to follow the human operator force F_h. First, we define the following variable:

$$G_s''\left(s\right) = \frac{G_s'\left(s\right)}{1+C_s\left(s\right)G_s'\left(s\right)} \quad (15)$$

Then, Figure 2 can be simplified as in Figure 6. Now, since sending the contact force through the reflection path of communication channel performs the force tracking, a new output in the block diagram of Fig. 6 can be defined as F_r. Hence, the structure of local master controller design can be redrawn as in Figure 7. In Figure 7, W_{m2} is the uncertainty weighting function related to the time delay introduced in section 2.2 and W_{pm} and W_{um} are the performance and controller weighting functions which are chosen based on

objectives of the local master controller design (characteristics of the time response and maximum value of the control signal). Consequently, the local master controller C_m can be constructed from Theorem 2.
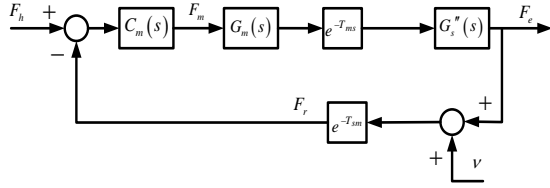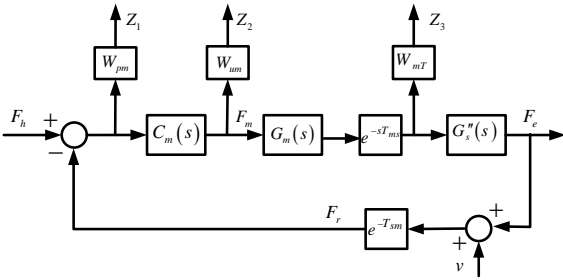

Figure 6. The closed-loop structure

Figure 7. The structure of local master controller design.

Theorem 2: Consider the closed-loop control system in Figure 7. The local master controller with tracking error bound γ would exist if there exist X and Y that can satisfy the minimization of the following convex optimization inequality [33]:

$$mininmize \; \gamma \qquad (16)$$

$$Subject \; to \begin{pmatrix} \Lambda_{11} & 0 \\ 0 & \Lambda_{22} \end{pmatrix} < 0, \begin{pmatrix} X & I & * \\ I & Y & * \\ M_{31} & M_{32} & Q \end{pmatrix} > 0$$

$$, Tr(Q) < \nu, \; D_{z_2 w} + D_{z_2} \hat{D}_k D_w = 0$$

where Π_{11}, Π_{21}, Π_{31}, Π_{22}, Π_{41}, Π_{32}, Π_{42}, Π_{43} introduced in (12) and

$$\Lambda_{11} = \begin{pmatrix} \Pi_{11} & * & * & * \\ \Pi_{21} & \Pi_{22} & * & * \\ \Pi_{31} & \Pi_{32} & -\gamma I & * \\ \Pi_{41} & \Pi_{42} & \Pi_{43} & -\gamma I \end{pmatrix} \qquad (17)$$

$$\Lambda_{22} = \begin{pmatrix} \Pi_{11} & * & * \\ \Pi_{21} & \Pi_{22} & * \\ \Pi_{31} & \Pi_{32} & -I \end{pmatrix}$$

$$M_{31} := C_{z_2} X + D_{z_2} \hat{C}_k$$

$$M_{32} := C_{z_2} + D_{z_2} \hat{D}_k C$$

where * and the variables A, B_w, C_z, D_{zw}, $A\Box_k$, $B\Box_k$, $C\Box_k$ and $D\Box_k$ have been introduced before.

5. Simulation results

The one-degree of freedom manipulator is used for the master and the slave systems similar to many papers in this field [34]. The dynamic equation of the master and the slave systems are considered as

$$\frac{y_m}{u_m} = \frac{1}{M_m s^2 + B_m s} \qquad m_{min} \le M \le m_{max}$$
$$b_{min} \le B \le b_{max} \qquad (18)$$
$$\frac{y_s}{u_c} = \frac{1}{M_s s^2 + B_s s} \qquad z_{emin} \le Z_e \le z_{emax}$$

Where B is the viscous friction coefficient, M is the mass, u is the input, Z_e is the impedance of the environment and indices m and s are for the master and the slave, respectively. The parameter values are given in Table 1. To evaluate the effectiveness of the proposed method in the presence of model mismatch, simulations are carried out for three cases:

Case 1: The time delay uncertainty.

Case 2: The time delay uncertainty and the parameter uncertainty in the slave system.

Case 3: The time delay uncertainty as well as the parameter uncertainties in the slave system and the task environment.

Table 1. System parameters

Symbol	Amount
M_m	1.5
B_m	11
m_{min}	0.1
m_{max}	3.9
b_{min}	3
b_{max}	27
T_{min}	0
T_{max}	3
Z_e	2
z_{emin}	1
z_{emax}	3
K_p	1
K_f	1

In simulations, two different inputs, which are the most common and generic dynamic test for control scheme, are utilized in simulations; step input and sinusoidal input. As a result, the control performance is evaluated by applying a step and a sinusoidal force exerted by human operator. It is necessary to recall that a large time delay is considered in the simulation. The time delay in bilateral teleoperation systems is defined small for $T \le 0.001 \; sec$ [25], [26]. As it mentioned in section 2 in part B, the parameter α is set to 0.5. In all cases, the multiplicative uncertainty weight for time delay given in (7.2).

$$W_{mT}(s) = \frac{1.5s}{0.4329s + 1} \qquad (19)$$

As shown in Figure 8, the opted weighting functions can cope with the time delay uncertainties and the variation of parameters in the slave system. The corresponding weighting functions depicted in Figures 5 and 7 are given in Table 2 and 3, respectively. Moreover, Table 4 represents the obtained local controllers in different cases. From Theorem 1, to reduce the effect of uncertainty in the parameters of slave system and task environment in both Case 2 and Case 3, a bounded peak-to-peak gain controller (i.e. local slave controller C_s) in the remote site is employed. In addition, from the generalized structure given in (8) and Theorem 2, the local master controller C_m is obtained. Recall that the reduced order of local master controllers C_m using Normalized Coprime Factorization (NCF) method is given in Table 4.

Simulation results are shown in Figures 9-13. These figures are the human force, the transparency response (position and force tracking), and the controller signals. Recall that force tracking error is a difference between human operator force f_h and reflected force f_r in presence measurement noise, whereas position tracking error is a difference between position of master x_m and slave x_s. From these figures, it can be seen that the designed controllers can meet the objectives i.e. robust stability and complete transparency. Furthermore, the local master controller can reduce the measurement noise accompanied by the reflected force from remote environment. Finally, to show the stability and performance index of the system in presence of model mismatch, μ analysis is used. Figures 13a and 13b illustrate the μ bound of the closed-loop stability and performance with designed local controllers. Since the values of μ bound related to the stability of system is smaller than one and near one for the performance, the designed controllers preserve the robust stability in presence model mismatch while the performance of system does not change effectively.

6. Conclusion

To achieve robust stability and complete transparency, this paper proposed a novel LMI-based robust control design for bilateral teleoperation systems in presence of uncertainties in time delay in communication channel, task environment and model parameters of master-slave systems, which is called model mismatch. Methodology in this paper focused on the time delay in communication channel assumed to be large and unknown, but the upper bound of the delay was assumed to be known. This assumption is very general for the time delay in communication channel. Two local controllers: One on the master side and the other one on the slave side were designed. The slave controller guarantees the position tracking and the master controller guarantees force tracking as well as the robust stability of the overall closed-loop system. Simulation results show the feasibility of the proposed control method. Future works in this research domain will include considering unbounded time delay in communication channel for proposed structure and some analytical and practical work and conditions for stability robustness of the closed-loop system.

Table 2. Corresponding weighting function for local slave controller design shown in Figure 5

Weighting Function	Case 1	Case 2	Case 3
$W_{ps}(s)$	–	1	1
$W_{us}(s)$	–	$W_{us2} = 0.001$	$W_{us3} = 0.008$
$W_{ms}(s)$	–	$W_{ms2}(s) = \dfrac{18.05(s+1.035)}{s+5.499}$	$W_{ms3}(s) = \dfrac{17.352\ (s+0.07123)}{s+2.759}$

Table 3. Corresponding weighting function for local master controller design shown in Figure 7

Weighting Function	Case 1	Case 2	Case 3
$W_{pm}(s)$	$\dfrac{0.065}{s + 0.0001}$	$\dfrac{0.065}{s + 0.0001}$	$\dfrac{0.065}{s + 0.0001}$
$W_{um}(s)$	0.0001	0.0001	0.0001
$W_{mT}(s)$	$\dfrac{1.5s}{0.4329s + 1}$	$\dfrac{1.5s}{0.4329s + 1}$	$\dfrac{1.5s}{0.4329s + 1}$

Table 4. Local controllers

Cases	Local master controller	Local slave controller
Case 1	$C_{m_1} = \dfrac{5.2221(s+0.7381)(s^2+7.429s+41)}{(s+3.02)(s+1.293)(s^2+4.963s+49.57)}$	$C_{s_1}(t) = \dfrac{82.22s+10.9603}{s}$
Case 2	$C_{m_2} = \dfrac{0.6378(s+15.05)(s+0.5056)(s+0.0002)}{(s+8.587)(s+0.0004)(s^2+1.576s+0.7693)}$	$C_{s_2} = \dfrac{2.97\times10^5(s+9.993)}{(s^2+123.4s+7088)}$
Case 3	$C_{m_3} = \dfrac{0.4805(s+89.52)(s+10.57)(s+0.0004)}{(s+4.608)(s+0.0008)(s^2+7.032s+130.5)}$	$C_{s_3} = \dfrac{6.35\times10^6(s+27.02)}{(s^2+378.1s+5.28\times10^4)}$
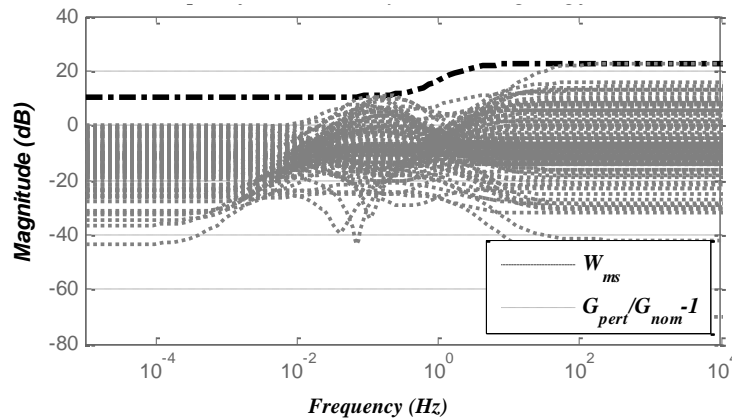
Figure 8a. Bode diagram of the weighting function W_{ms} for the uncertain slave system G/G_0-1
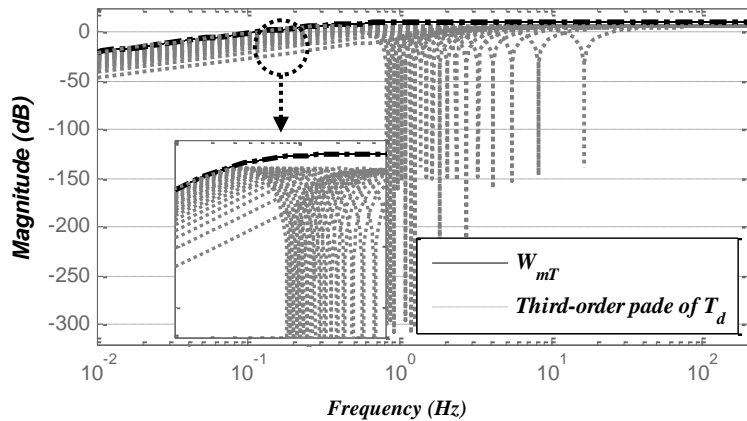
Figure 8b. Bode diagram of the multiplicative weight function W_{mT} for third order Pade´ approximation of time delay.
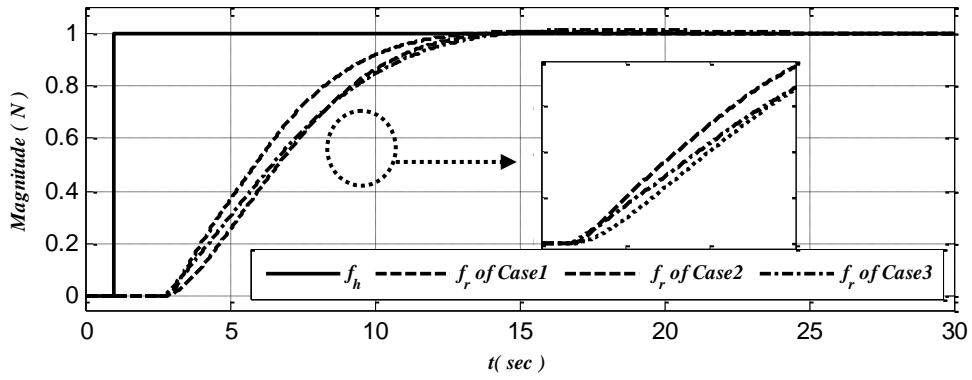
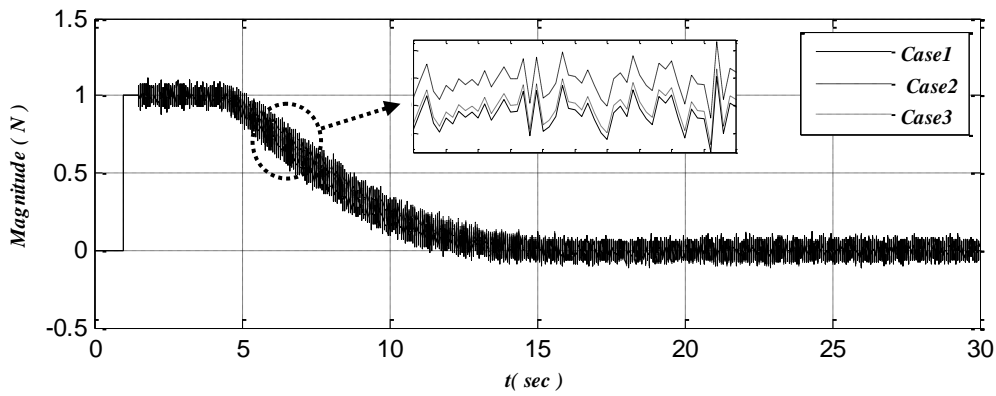**Figure 9a.** Force tracking for step input (Human operator F_h and reflected force F_r)

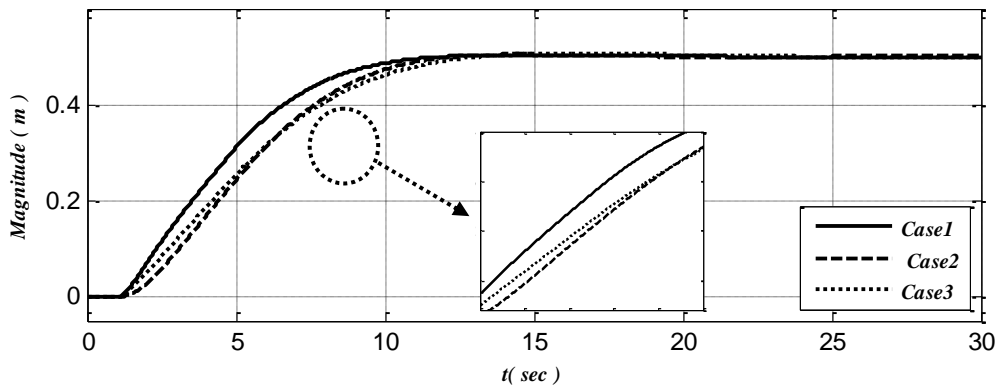**Figure 9b.** Force tracking error for step input

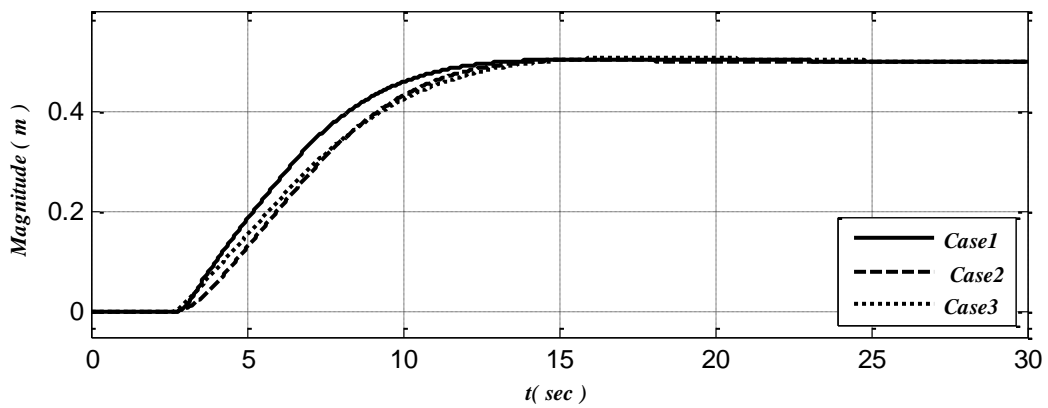**Figure 10a.** Position of master for step input (x_m)

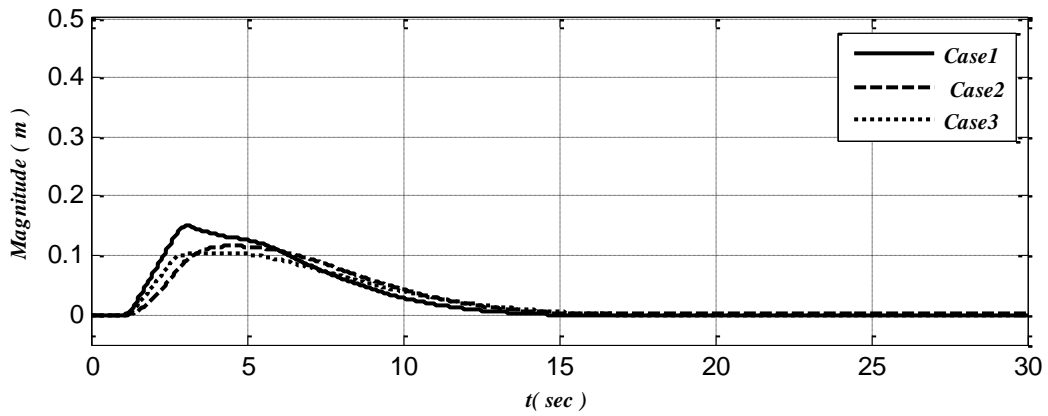**Figure 10b.** Position of slave for step input (x_s)

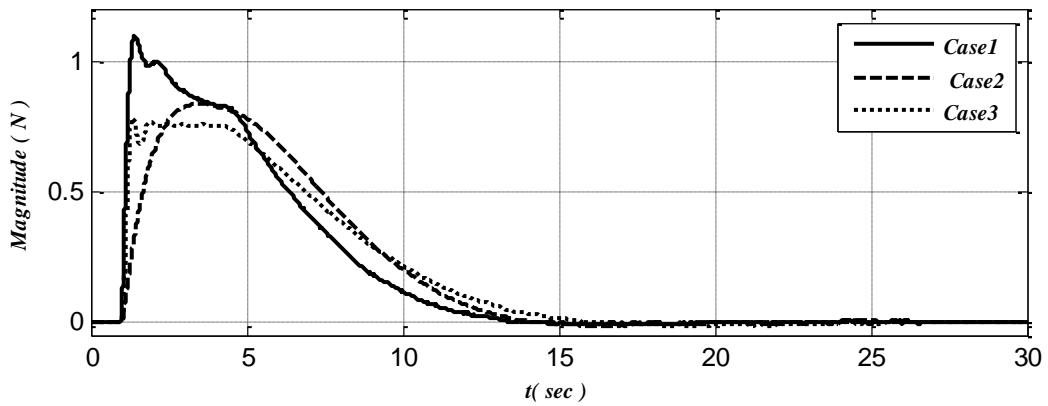**Figure 10c. Position tracking error for step input**

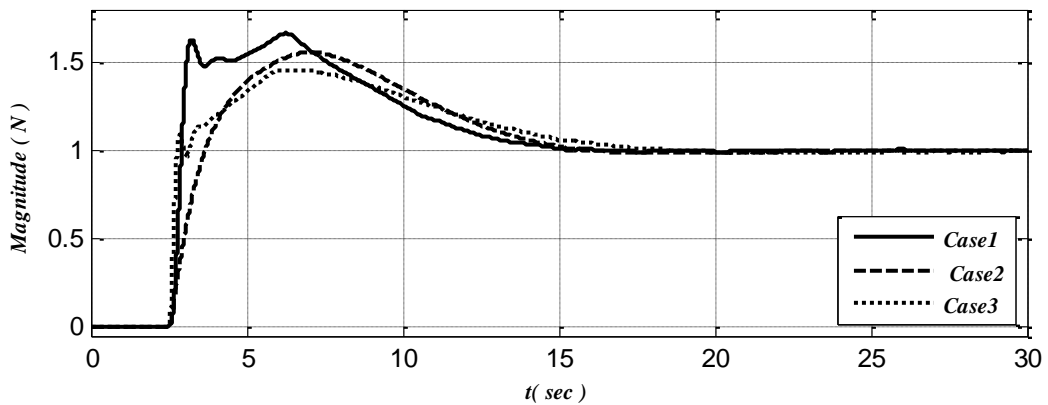**Figure 11a. Master controller signal for step input (f_m)**

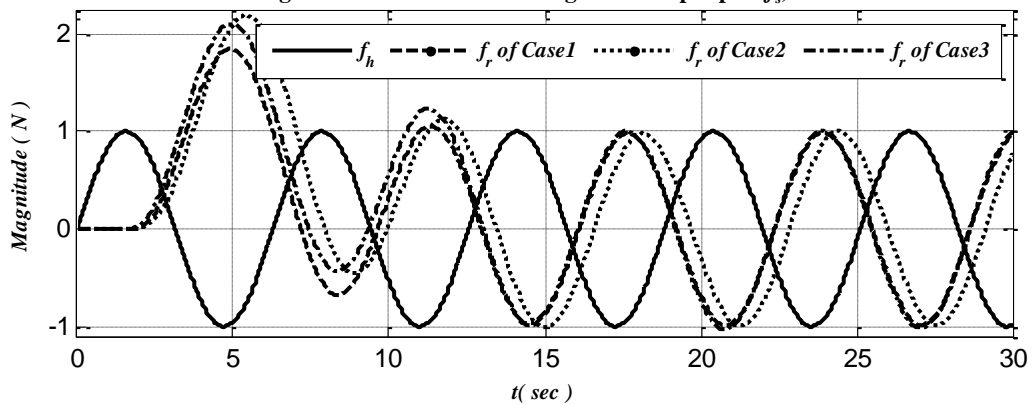**Figure 11b. Slave controller signal for step input (f_s)**

Figure 12a. Force tracking for sinusoidal input (Human operator F_h and reflected force F_r)
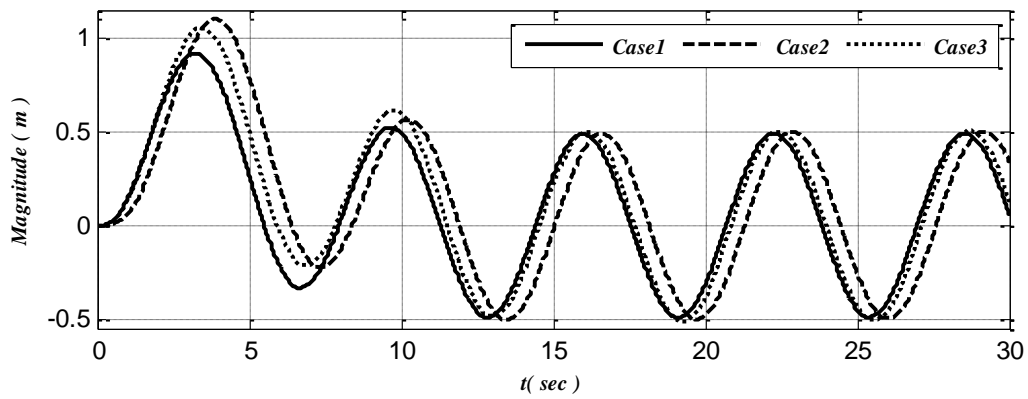
Figure 12b. Position of master system for sinusoidal input (x_m)
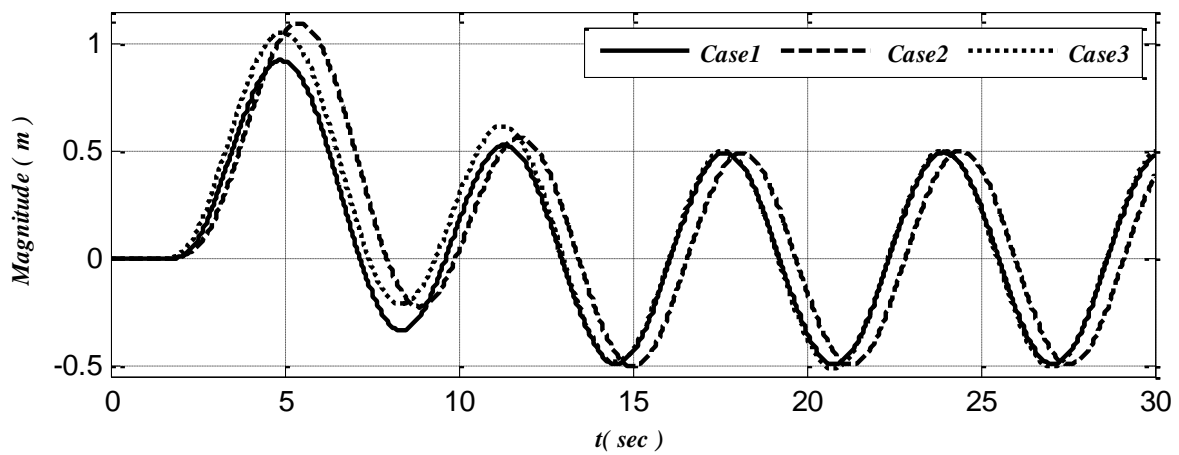

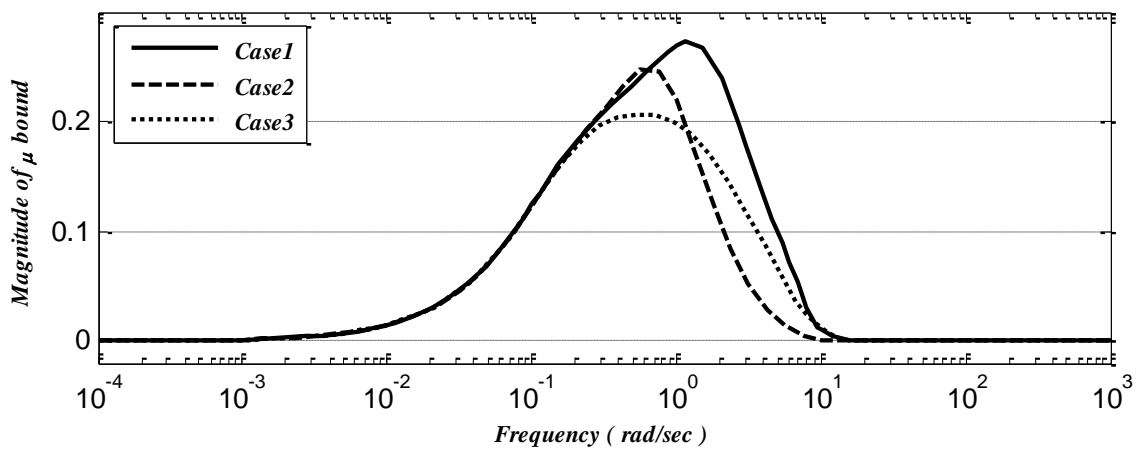**Figure 12c. Position of slave system for sinusoidal input (x_s)**

Figure 13a. μ bound of the closed-loop stability with designed local controllers
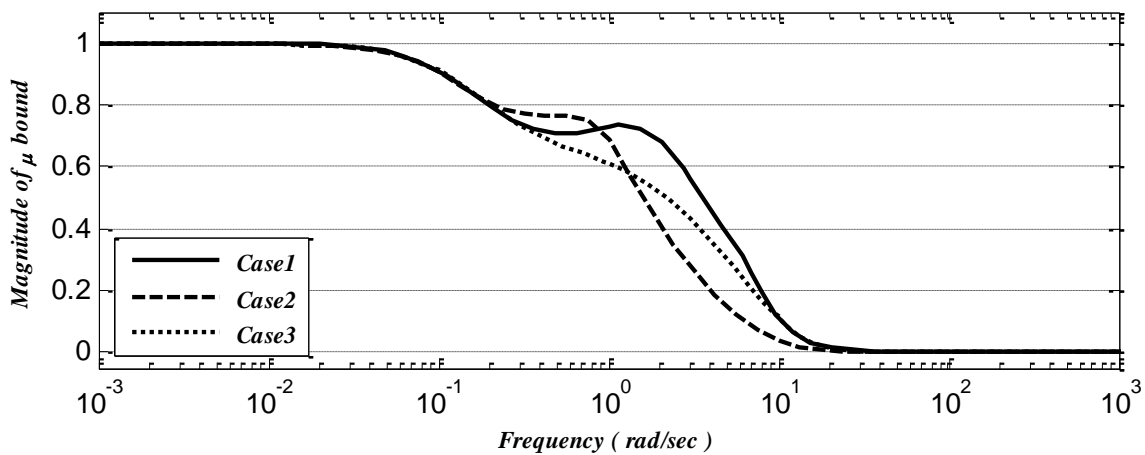
Figure 13b. μ bound of the closed-loop performance with designed local controllers

References

[1] Smith, A., Mobasser, F. and Hashtrudi-Zaad, K. (2006). Neural network based contact force observers for haptic applications. IEEE Transactions on Robotics. 22(6), 1163-1175.

[2] Lawrence, D. A. (1993). Stability and transparency in bilateral teleoperation. IEEE Transactions on Robotics and Automation. 9(5), 625-637.

[3] S. E. Salcudean, M. Zhu, W. H. Zhu, K. Hashtrudi-Zaad. (2000). Transparent bilateral teleoperation under position and rate control. Robotics Research. 19, 1185-1202.

[4] Hannaford. B. (1998). Stability and performance tradeoffs in bilateral telemanipulation. IEEE Conference on Robotics and Automation, 584-589.

[5] Ni, L. and Wang, D. W. L. (2002). A gain-switching control scheme for position-error-based force reflecting teleoperation. 10th IEEE Symposium Haptic Interfaces for Virtual and Teleoperator Systems.

[6] Kim, J., Chang, P. H. and Park, H. S. (2005). Transparent teleoperation using two-channel control architectures. Conference on Robotics and Automation. 2824-2831.

[7] Yokokohji, Y. and Yoshikawa, T. (1994). Bilateral control of master-slave manipulators for ideal kinesthetic coupling-Formulation and experiment. IEEE Transactions on Robotics and Automation. 10(5), 605-620.

[8] Garsia-Valdovinos, L. G., Parra-Vega, V. and Artega, M. A. (2007). Observer-based sliding mode impedance control of bilateral teleoperation under constant unknown time delay [J]. Robotics and Autonomous Systems. 55, 609-617.

[9] Cho, H. C. and Park, J. H. (2005). Stable bilateral teleoperation under a time delay using a robust impedance control. Mechatronics. 15, 611-625.

[10] Zhu, W. H. and Salcudean, S. E. (2000). Stability guaranteed teleoperation: An adaptive motion/force control approach. IEEE Transactions on Automatic Control. 45(11), 1951-1969.

[11] Lee, D. and Spong, M. W. (2006). Passive bilateral teleoperation with constant time-delay. IEEE Transactions on Robotics. 22(2), 269-281.

[12] Slama, T., Aubry, P., Vieyres, P. and F. Kratz. (2005).Delayed generalized predictive control of bilateral teleoperation systems. 6th IFAC World Congress, Prague.

[13] Arcara, P. and Melchiorri, C. (2002). Control schemes for teleoperation with time delay: a comparative study. Robotics and Autonomous Systems. 38, 49-64.

[14] Buttolo, P., Braathen, P. and Hannaford, B. (1994). Sliding control of force reflecting teleoperation: preliminary studies. Presence. 3(2), 158-172.

[15] Anderson, R. and Spong, M. W. (1989). Bilateral control of teleoperators with time delay. IEEE Transactions Robotics and Automation. 34(4). 494-501.

[16] Park, J. H. and Cho, H. C. (1999). Sliding-mode controller for bilateral teleoperation with varying time delay. IEEE Conference on Advanced Intelligent and Mechtronics. 311-316.

[17] García-Valdovinos, L. G., Parra-Vega, V. and Artega, M. A. (2007). Observer-based sliding mode impedance control of bilateral teleoperation under constant unknown time delay. Robotics and Autonomous Systems. 55(8), 609-617.

[18] Namerikawa, T. and Kawada, H. (2006). Symmetric impedance matched teleoperation with position tracking. IEEE Conference on Decision and Control. 4496-4501.

[19] Liu, X., Wilson, W. J. and Fan, X. (2005). Pose reflecting teleoperation using wave variables with

wave prediction. IEEE International Conference on Mechatronic and Automation. 1642-1647.

[20] Azorín, J. M., Reinoso, O., Aracil, R. and Ferre, M. (2004). Control of teleoperators with communication time delay through state convergence. Robotic Systems. 21,167-182.

[21] Ueda, J. and Yoshikawa, T. (2004). Force-reflecting bilateral teleoperation with time delay by signal filtering. IEEE Transactions on Robotics and Automation. 20(3), 613-619.

[22] Eusebi, A. and Melchiorri, C. (1998). Force reflecting telemanipulators with time-delay: stability analysis and control design. IEEE Transactions on Robotics and Automation. 14(4), 635-640.

[23] Oboe, R. and Fiorini, P. (1998). A design and control environment for internet-based telerobotics. Robotic research. 17(4), 433-449.

[24] Hashtrudi-Zaad, K. and Salcudean, S. E. (2002). Transparency in time-delayed systems and the effect of local force feedback for transparent teleoperation. IEEE Trans. Robotics Automation. 18(1), 101-114.

[25] Alfi, A. and Farrokhi, M. (2008). A simple structure for bilateral transparent teleoperation systems with time delay. Dynamic Systems, Measurement, and Control. 130(4), 1-9.

[26] Alfi, A. and Farrokhi, M. (2008). Force reflecting bilateral control of master-slave systems in teleoperation. Intelligent and Robotic systems. 52(2), 209-232.

[27] Gu, K., Kharitonov, V. L. and Chen, J. (2003). Stability of time-delay systems. Springer, Birkhusera.

[28] ShaSadeghi, M., Momeni, H. R. and Amirifar, R. (2008). H_∞ and L_1 control of a teleoperation system via LMIs. Applied Mathematics and Computation. 206, 669-677.

[29] Hua, C. C. and Liu, P. X. (2009). Convergence analysis of teleoperation systems with unsymmetric time-varying delays. IEEE Transactions Circuits System.-II: Express Briefs. 56(33), 240-243.

[30] Xu, B. and Liu, Y. H. (2009). Delay-dependent/delay-independent stability of linear systems with multiple time-varying delays. IEEE Transactions on Automatic Control. 48(4), 697-701.

[31] Filipiak. J. (1988). Modelling and control of dynamic flows in communication networks. Berlin: Springer.

[32] Goktas, F., Smith, J. M. and Bajcsy, R. (1996). μ-Synthesis For Distributed Control Systems with Network-Induced Delays. 35th Conference on Decision and Control. 813-814.

[33] Scherer, C., Gahinet, P. and Chilali, M. (1997). Multiobjective output-feedback control via LMI optimization. IEEE Transactions on Automatic Control. 42(7), 896-911.

[34] Hokayem, P. F. and Spong, M. W. (2006). Bilateral teleoperation: an historical survey. Automatica. 42,2035-2055.